Comparison of bacterial carbon production estimates from dilution and ^{3}H-leucine methods across a strong gradient in ocean productivity

Michael R. Landry [1]*, Sara R. Rivera [2], Michael R. Stukel [3], Karen E. Selph [4]

[1]Scripps Institution of Oceanography, University of California, San Diego, California
[2]Department of Earth and Environmental Sciences, University of Michigan, Ann Arbor, Michigan
[3]Earth, Ocean, and Atmospheric Science Department, Florida State University, Tallahassee, Florida
[4]Department of Oceanography, University of Hawai'i at Manoa, Honolulu, Hawaii

Abstract

The uptake of ^{3}H-labeled leucine into proteins, a widely used method for estimating bacterial carbon production (BCP), is suggested to underestimate or overestimate bacterial growth in the open ocean by a factor of 40 uncertainty. Meanwhile, an alternative BCP approach, by the dilution method, has untested concerns about potential overestimation of bacterial growth from dissolved substrates released by filtration. We compared BCP_{Dil} and BCP_{Leu} estimates from three cruises across a broad trophic gradient, from offshore oligotrophy to coastal upwelling, in the California Current Ecosystem. Our initial analyses based on midday microscopical estimates of bacterial size and a priori assumptions of conversions relationships revealed a mean two-fold difference in BCP estimates (BCP_{Dil} higher), but no systematic bias between low and high productivity stations. BCP_{Dil} and BCP_{Leu} both demonstrated strong relationships with bacteria cell abundance. Reanalysis of results, involving a different cell carbon-biovolume relationship and informed by forward angle light scatter from flow cytometry as a relative cell size index, demonstrated that BCP_{Dil} and BCP_{Leu} are fully compatible, with a 1 : 1 fit for bacteria of 5 fg C cell^{-1}. Based on these results and considering different strengths of the methods, the combined use of ^{3}H-labeled leucine and dilution techniques provide strong mutually supportive constraints on bacterial biomass and production.

The rate of tritiated leucine (^{3}H-leucine) uptake into proteins in short-term assays is a standard and widely used method for estimating carbon production by heterotrophic prokaryotes (hereafter, bacterial carbon production, BCP) (Kirchman et al. 1985; Simon and Azam 1989; Smith and Azam 1992; Ducklow 2000; Kirchman 2001). In principle, BCP can also be estimated from the net growth rates of heterotrophic prokaryotes (hereafter, bacteria) measured in seawater dilution experiments (Landry and Hassett 1982) by the same techniques that have been applied to phototrophic microbes like *Prochlorococcus*, *Synechococcus*, and picoeukaryotes (Landry et al. 1995, 2003, 2022; Selph et al. 2011). Rate estimates for bacteria appear in some of the earliest dilution studies (Landry et al. 1984) but have been relatively few in comparison to those for photosynthetic populations (Calbet and Landry 2004; Schmoker et al. 2013). This is partly explained by the wide use of chlorophyll *a* as the measurement variable for phototrophs, which has no equivalent for bacteria. It also stems from the fact that the growth environment (temperature, light, and nutrients) for photosynthetic microbes is relatively easy to maintain during dilution incubations, whereas the specific organic substrates required for bacterial growth are more difficult to assess or control. Treatment biases could occur, for example, if the filtration process to produce water for the dilution treatment(s) enriches the filtrate with higher levels of organic substrates than in undiluted water (Fuhrman and Bell 1985; Pree et al. 2016). Given the complexities of dissolved organic substrate composition in seawater, whether specific molecules are labile or recalcitrant and how they relate to the substrate requirements and quotas of diverse bacterial assemblages, it is not likely that such an issue can be definitively resolved for all systems or conditions. We can, however, ask, as we do here, how do estimates of bacterial production from a meaningful

sampling of dilution experiments over varying environmental conditions compare to the ³H-leucine BCP standard?

Beyond a simple method comparison, the answer to the above question is also relevant to important contemporary issues of bacterial ecology and rate assessments in the oceans. Recent studies, for example, have strongly questioned whether bacteria growth rate estimates from ³H-leucine are reliable for open-ocean ecosystems, with Popendorf et al. (2020) indicating that they may be a factor of 7 too low and Giering and Evans (2022) suggesting that they could be a factor of 6 too high. The population-focused approach of the dilution method, using measured changes in cell abundances as the basis for rate calculations, provides a more direct determination of bacteria cell growth rates than ³H-leucine and is therefore relevant to addressing this 40-fold range of uncertainty. Whether dilution results support or differ greatly from those of ³H-leucine may therefore contribute to the discussion of these issues. Dilution experiments also differ from ³H-leucine assays in their potential to compare the vital rates of different microbial populations to one another in the same incubations. Therefore, if dilution results are compatible to ³H-leucine for bacteria in aggregate, the population-distinguishing advantage of dilutions could be useful as a tool for integrating bacterial production into food web studies relative to phototrophic microbes as well as for using molecular sequence techniques to quantify potential differences and growth-mortality tradeoffs among co-occurring microbes (Yokokawa and Hagata 2005; Cheung et al. 2022).

In the present study, we examine BCP results from dilution and ³H-leucine experiments conducted on three process cruises of the California Current Ecosystem-Long-Term Ecological Research (CCE-LTER) Program. The CCE cruises were not specifically structured to test or compare methods, but rather to investigate system-level behavior, including community composition and process relationships, across a large gradient of ecological conditions from coastal upwelling to offshore oligotrophy. The broad productivity range among experimental sites is thus a unique and important feature of the data that are compared, as is the Lagrangian cruise design of following a satellite-tracked drifter to minimize advective bias and maintain natural in situ conditions of temperature and light for dilution incubations. In other respects, however, the two types of experiments were conducted and analyzed independently according to their own a priori protocols. We first compare these raw results for experiments that match closely by sampling day and depth. In discussion, we consider all of the factors that might cause results to differ and how they can be reconciled.

Materials and procedures

Bacterial rate measurements were made by methodologically consistent applications of ³H-leucine and seawater dilution techniques on three process cruises of the CCE-LTER Program in August 2014 (P1408), April 2016 (P1604)

and August 2017 (P1708). Each cruise examined ecological processes at 4–5 locations spanning the CCE's strong onshore-offshore productivity gradient (Morrow et al. 2018; Kranz et al. 2020; Valencia et al. 2022). At each site, we conducted 2–4 d experiments during which process rate profiles were done each day on a rigorously repeated time schedule optimized for each method while following a satellite-tracked drifter with a 3-m drogue at 15 m (Landry et al. 2009). Water for dilution experiments was sampled at six depths spanning the euphotic zone from CTD hydrocasts conducted at 02:00 local time. Following set-up procedures, the dilution experiments were initiated before sunrise and incubated in situ for 24 h in coarse net bags attached to a line below the drift array at the depths of CTD sample collection. Water samples for ³H-leucine uptake experiments were collected at 4–8 depths from CTD hydrocasts at 11:00 local time in close proximity to the drift array and incubated for one-hour duration on shipboard. According to this quasi-Lagrangian sampling plan, we compare predawn-to-predawn dilution incubations under ambient temperature and light conditions to short-term mid-day ³H-leucine experiments incubated separately, but from the same photo-day and water parcel without the potential vagaries of large advective bias.

Dilution setup and protocols

For each experimental day, we set up a depth profile of dilution experiments from water collected at six depths spanning the euphotic zone (nominally, the depth of penetration of ~ 1% surface irradiance). For each depth, a two-treatment dilution experiment (Landry et al. 2008, 2011) was prepared, with one polycarbonate bottle (2.7 L) containing unfiltered seawater (100%) and the second (diluted) bottle consisting of ~ 33% whole seawater with filtered water from the same depth. Seawater was filtered directly from the Niskin bottles using a peristaltic pump, silicone tubing and in-line 0.1-μm Suporcap filter capsules that had previously been acid washed. Dilution bottles were first given a measured volume of filtered water and then filled gently to the top with unscreened water from the Niskin bottles to avoid physical damage to fragile protists. During the filling process, we alternated volume allocations between the two bottles so that any vertical stratification of population abundances in the Niskin bottles would be distributed equally between the diluted and undiluted treatments. Consistent with previous studies (Landry et al. 2008, 2011, 2022), nutrients were not added to the incubation bottles to avoid suppression of grazing in oligotrophic waters (Lessard and Murrell 1998). Each filled bottle was subsampled for flow cytometry (FCM) analysis (1–2 mL, preserved with 0.5% paraformaldehyde and flash frozen in liquid nitrogen) for initial bacterial concentrations.

All bottles were placed in coarse net bags, attached to the line below the drifter float and incubated in situ for 24 h at the depths of collection. For back-to-back daily experiments, the new experiments were set up in net bags on deck before

hand-recovery of the drifter. The previous day's experiments were then removed, the new experiments attached, and the drifter redeployed—a process that took 10–15 min while the ship maintained position. Sampling for daily experiments was done in close proximity (~ 100 m) to the drifter position, and all recovery and deployments were carried out before sunrise.

Upon recovery, FCM subsamples were immediately taken from each bottle after gentle mixing for measurement of final bacteria abundances. On shore, the samples were stored at $-80°$C, then thawed in batches and stained with Hoechst 33342 (1 μg mL^{-1}, final concentration) immediately prior to analysis (Monger and Landry 1993). The analyses of initial and final FCM samples were done using a Beckman-Coulter Altra flow cytometer equipped with a Harvard Apparatus syringe pump to quantify volume sampled and two argon ion lasers tuned to UV (200 mW) and 488 nm (1 W) excitation. Fluorescence signals were collected using filters for Hoechst-bound DNA, phycoerythrin and chlorophyll; all normalized to bead standards of 0.5- and 1.0-μm yellow-green (UV or YG) polystyrene beads. Listmode files were analyzed with FlowJo software to obtain concentrations of heterotrophic bacteria based on DNA signal (all cells), absence of photosynthetic pigments (heterotrophs), and forward angle light scatter (FALS; relative size).

Calculating BCP estimates from dilution experiments

For each dilution experiment of 1 d duration ($t = 1.0$), we computed the net growth rates of bacteria from initial and final FCM cell abundances in diluted (k_d) and undiluted (k) treatments as:

$$k = \ln\left(P_t/P_0\right) \text{ and } k_d = \ln\left(P_{t,d}/(D \times P_0)\right) \tag{1}$$

where P_t and $P_{t,d}$ are final bacteria cells mL^{-1} in undiluted (control) and diluted treatments, respectively, and P_0 is initial abundance in the undiluted treatment. We used subsamples of initial bacteria concentrations in the diluted treatments ($P_{0,d}$) only to determine a mean dilution factor D from the ratio of $P_{0,d}$ to P_0, which was done for all experiments on each cruise separately. We then applied the same average ratio to all experiments for the cruise. This is done to avoid transferring random subsampling errors in measuring $P_{0,d}$, due to incomplete mixing of natural and filtered waters during the filling and subsampling process, to the rate calculations. For heterotrophic bacteria, we found that the mean measured D was very close to but slightly higher than the intended D defined by the relative volumes of filtered and natural waters. The difference was equivalent to the passage of $\sim 1\%$ of bacterial cells through a 0.1-μm filter cartridge. In contrast, mean measured values of D for phototrophic bacteria, *Prochlorococcus* and *Synechococcus*, in the same experiments were not different from the calculated relative volume ratio (intended D). Such differences can have meaningful impacts on dilution rate calculations and are likely to be larger for the

coarser filters (0.2-μm and higher) used more generally in experimental setups. To avoid systematic bias in comparing the relative rates of different populations in the same experiments, an effective D should be established for each group, or at least up to size classes that are removed 100% by the filters.

Rate estimates for bacterial grazing mortality (m, d^{-1}) and instantaneous growth (μ, d^{-1}) were calculated from the two-treatment equations of Landry et al. (2008, 2011):

$$m = (k_d - k)/(1 - D) \text{ and } \mu = k + m \tag{2}$$

Carbon-based estimates of bacterial production (BCP$_{Dil}$) were determined as the product of bacterial growth rate and biomass. For the special case of $k = 0$ for a 24-h incubation (i.e., $\mu = m$; $t = 1$),

$$BCP_{Dil} = \mu \times C_B \times P_0 \tag{3}$$

where C_B is the carbon content of an individual bacteria cell. For $k \neq 0$ or for t different from 1 d, we applied the more general equation (Landry et al. 2003) for time averaging the increases or decreases in P during the incubation period:

$$BCP_{Dil} = \mu \times C_B \times P_0 \times \left(e^{kt} - 1\right)/kt \tag{4}$$

For the present method comparison, we also define a minimum value of BCP, here BCP$_{Min}$, determined from the observed changes in bacterial abundances in undiluted bottles over the one-day incubations. BCP$_{Min}$ cannot be a negative number. Therefore, when measured net growth rates were negative ($k \leq 0$), we set BCP$_{Min}$ to zero or to a nominally low value (0.01 mg C m^{-3}) in order to visualize those points on log-scale plots. For all experiments in which $k > 0$, BCP$_{Min}$ is the net measured biomass increase:

$$BCP_{Min} = C_B \times P_0 \times \left(e^{kt} - 1\right) \tag{5}$$

BCP estimates from ^{3}H-leucine

BCP$_{Leu}$ estimates were determined according to the short-term incubation and centrifugation method described by Smith and Azam (1992). For each depth sampled from 11:00 CTD hydrocasts, triplicate live assays and one TCA-killed control (5% trichloroacetic acid) were prepared by adding 1.7 mL of seawater to sterile 2-mL microcentrifuge tubes then adding ^{3}H-leucine (L-leucine, [4,5-3H], Moravek, Inc MT672; specific activity = 5 TBq mmol^{-1}) to achieve final concentrations of 20 nM. The samples were incubated in dark, temperature-controlled incubators. Following incubation, the live assays were killed by adding 100% TCA for a final concentration of 5% TCA. The samples were centrifuged at 16,000 $\times$ *g* for 10 min, decanted and washed with the addition of 1.5 mL of 5% TCA. This was followed by re-centrifugation (16,000 $\times$ *g* for 10 min), decantation, drying the samples, and addition of

scintillation cocktail (0.5 mL; Ultima Gold, PerkinElmer). Samples were frozen and stored at $-20°C$ as necessary. After at least 24-h incubation in scintillation cocktail at room temperature, disintegrations min^{-1} were read on a Beckman LS6000A liquid scintillation counter and converted to carbon synthesis rates (mg m^{-3} d^{-1}) using the theoretical CF_{Leu} of 3.1 kg C mol^{-1} leucine (Simon and Azam 1989) and assuming the same hourly production rates over full 24-h days.

Cellular carbon estimates for bacteria

On cruises P1604 and P1708, we collected seawater samples for microscopical analyses of bacterial cell sizes and biomass from the CTD hydrocast used for BCP_{leu} assays. These samples (3 mL preserved with 25% glutaraldehyde and 1% final concentration) were frozen in liquid N_2 and stored at $-80°C$ until analysis (< 3 months). Defrosted samples were filtered onto 25-mm polycarbonate filters of $0.22-\mu m$ pore size backed by 0.45 Millipore filters. The filters were dried at room temperature, and mounted using VECTASHIELD with DAPI (4′,6-diamindino-2-phenylindole) staining to highlight cell DNA, and imaged at 100X magnification on a Nikon C1 microscope. Images were analyzed with Nikon Advanced Research 3.2 software, and either 20 image fields or 200 cells $filter^{-1}$ were measured for lengths and widths with signal thresholding and length line cutoffs of $0.2–2.0$ μm to exclude nonbacteria cells.

Cell biovolumes (BV) were computed from measured lengths (L) and widths (W) as:

$$BV = \pi/4 \times W^2 \times (L - W/3) \qquad (6)$$

(Bratbak 1985). Cell carbon contents (C_B) were calculated as in Simon and Azam (1989):

$$C_B = 0.86 + 88.6 \times BV^{0.59} \qquad (7)$$

Given the lack of cell carbon data for cruise P1408, as well as the possibility that bacterial cell sizes could be substantially larger during the peak mid-day period of dissolved matter production by primary producers than at the predawn time of the dilution experiments, we used the microscopically measured cell sizes selectively, mainly to set the range for cell C contents that would apply across the spectrum of CCE productivity from rich coastal waters to oceanic oligotrophy. The sites of the highest productivity waters on P1604 and P1708 yielded 23 estimates of bacterial cell C, with a mean ($\pm$standard errors of the mean, SEM) value of 10.9 ± 0.6 fg C $cell^{-1}$ and a median value of 11.1 fg C $cell^{-1}$. Since both of these sites were absent the potential confounding influence of *Prochlorococcus* presence on bacterial cell sizing, we set 11 fg C $cell^{-1}$ as our estimate of C_B for high productivity waters (surface primary productivity > 100 mg C m^{-2} d^{-1}).

Because *Prochlorococcus* was a substantial fraction of the total number of bacteria-sized cells that would be counted by DAPI stain microscopy, with their larger cell sizes likely biasing the results, we subtracted their contribution from the P1604 experimental site chosen to be representative of low productivity waters (surface primary productivity <10 mg C m^{-2} d^{-1}). We did this by first multiplying the total abundance of heterotrophic bacteria and *Prochlorococcus* cells from FCM analyses times the microscopy cell size estimate to get a total biomass of bacteria. Then, we subtracted the biomass of *Prochlorococcus* cells (cell abundance × 32 fg C $cell^{-1}$; Garrison et al., 2000) from the total, and finally divided the remaining biomass by the abundance of heterotrophic bacteria in the FCM counts to get average cell C $bacteria^{-1}$. This yielded 10 estimates of cell C with mean ($\pm$SEM) and median values of 8.0 ± 0.5 and 8.0 fg C $cell^{-1}$, respectively.

Comparisons of BCP_{Dil} and BCP_{Leu}

Dilution experiments and ^{3}H-leucine assays are undertaken for different reasons on CCE Process cruises, with the former concentrated and more numerous in the euphotic zone and the latter sparser in the euphotic zone while extending deeply into the mesopelagic. To compare BCP rate estimates, we matched individual experiments where the depths of sample collection agreed closely and otherwise averaged the results of two closely spaced dilution experiments that had a BP_{Leu} estimate in the depth interval between them. A total of 127 production estimates are compared from the surface (2 m) to a maximum depth of 100 m, with a mean ($\pm$ std dev) depth of 26 ± 24 m. All regression analyses were done using the R *lmodel2* (version 1.7–3) package (Legendre 2022). Regression data described below are listed in Table S1, and relevant environmental data are available by cruise, CTD number and sampling depth at CCE data website https://oceaninformatics.ucsd.edu/datazoo/catalogs/ccelter/datasets.

Assessment

Figure 1 directly compares the matched BCP values from dilution experiments and ^{3}H-leucine incubations to one another by both reduced major axis (RMA, Model II) and ordinary least squares (OLS, Model I) regression models. Two BCP_{Dil} values that arose from negative rate estimates are plotted at 0.01 mg C m^{-3} d^{-1} for completeness but are excluded from the regression analyses. The regression relationships are equally significant for both models ($r = 0.700$; $p < 10^{-18}$) and have slopes (B) in the power function $Y = A \times X^B$ format not different from 1.0. For the RMA regression, $B = 1.14$ (0.94, 1.36), with lower and upper 95% confidence limits in parenthesis. For OLS, $B = 0.88$ (0.72, 1.04). However, BCP_{Dil} estimates are generally higher than BCP_{Leu}, as indicated by the regression offset from the 1 : 1 line. Intercept (A) values are 1.88 (1.66. 2.09) and 2.16 (1.79, 2.61), respectively, for the RMA and OLS models.

We investigated possible explanations and factors relevant to the observed rate offset in several ways. In Fig. 2, for example, we questioned whether systematic diel differences in
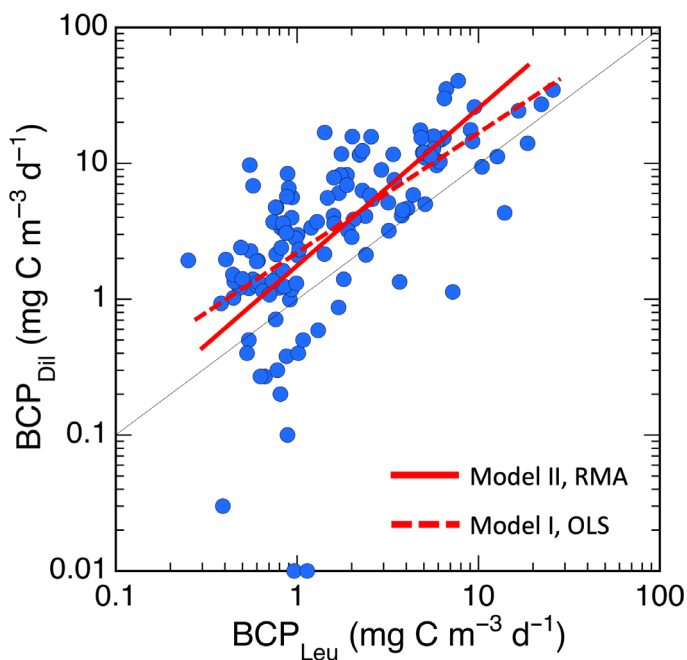
Fig. 1. Comparison of rate estimates of BCP determined from dilution incubations and ^{3}H-leucine uptake assays in the California Current Ecosystem. Regression models are RMA and OLS. The two points plotted at $BCP_{Dil} = 0.01$ mg C m^{-3} d^{-1} are from experiments with negative rates and are not included in the regressions.

bacterial cell abundances might underlie the rate differences by plotting BCP values from dilutions and leucine incubations relative to their respective FCM cell estimates from 02:00 to
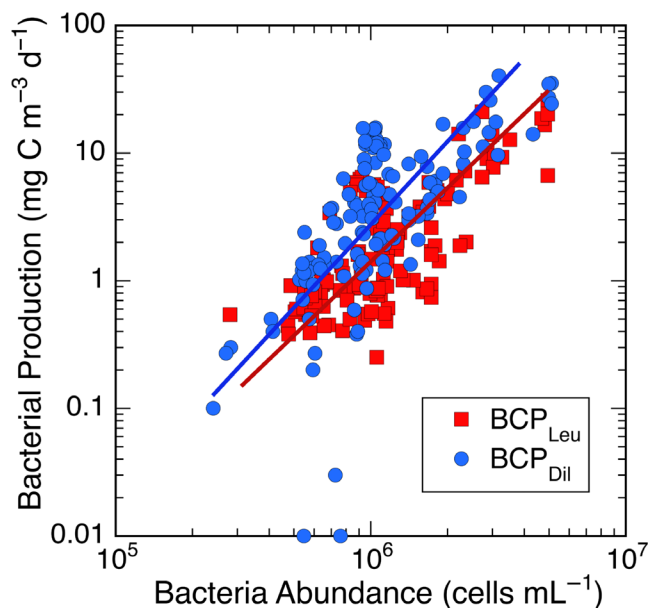

Fig. 2. Relationships of BCP determined from dilution incubations and ^{3}H-leucine uptake assays in the California Current Ecosystem relative to bacteria cell abundance. Regression lines are Model II (RMA). The two points plotted at $BCP_{Dil} = 0.01$ mg C m^{-3} d^{-1} are from experiments with negative rates and are not included in the regressions.

11:00 hydrocasts. Overall, mean ($\pm$ SEM) cell abundances were virtually identical in predawn ($1.31 \pm 0.09 \times 10^6$ cells mL^{-1}) and mid-day ($1.35 \pm 0.09 \times 10^6$ cells mL^{-1}) samplings, with variability mainly due to small-scale patchiness following the drogued drifter. Thus, there is no evidence that diel cycles in cell abundance affected the rate comparison. Nonetheless, the analysis demonstrates strong relationships ($p < 10^{-21}$) between BCP rates and abundance by both methods. Statistical tests of slope and intercept differences for RMA regressions of the log-transformed variables were conducted by non-parametric boot-strapping, sampling with replacement. The slopes (2.17 for BCP_{Dil}; 1.90 for BCP_{Leu}) are significantly different at $p = 0.0087$ (0.05, one-sided), and the intercepts (2.93×10^{-13} vs. 5.23×10^{-12}, respectively) differ at $p = 0.017$.

To determine if BCP rate estimates varied with system richness in a systematic manner, we divided the data into three groups of near-surface primary production (PP): PP < 10, 10 < PP < 100, and PP > 100 mg C m^{-3} d^{-1}, where PP is the measured mean of ^{14}C-uptake rates in triplicate bottles incubated in situ on the same drift arrays and depths as the dilution experiments (Table 1). Surface values of PP varied over more than two orders of magnitude, from 2 to 749 mg C m^{-3} d^{-1}, at individual stations, and from 3 to 133 mg C m^{-3} d^{-1} in the overall grouped means that included the lower values (due to diminishing light) in the deeper euphotic zones at each station. Substantial differences in the relative estimates of BCP_{Dil} and BCP_{Leu} are not evident among the groups, all of which indicate that dilution rates are higher by about a factor of 2. Bacterial growth rate (μ) estimates from dilution experiments vary from 0.23 to 0.62 d^{-1} for poorer to productive waters. For waters of low to intermediate productivity, grazing mortality rates closely match growth on average, such that population abundances remain stable in experimental bottles (net growth $k \approx 0$), as in the ambient ocean. For the richer waters, we observe small net growth of bacteria in the bottles,, which might be explained on balance by the exclusion of large metazoan consumers of bacterial-sized particles, principally pelagic tunicates, which can be abundant in the system, or by the sinking export of particle-attached bacteria.

To further understanding of the sensitivity of the regression relationship between BCP_{Dil} and BCP_{Leu} to assumptions of bacterial cell carbon content (C_B), we recalculated BCP_{Dil} results by applying C_B values of 7 to 13 fg C cell^{-1} to all experiments (i.e., $\pm 30\%$ around the intermediate value of 10 fg C cell^{-1} that we applied in the rate comparison, Fig. 1) and rerunning the regressions. The summary of that analysis in Fig. 3 shows that all uniformly applied values of C_B return a slope ($B = 1.03$, RMA) very close to and not significantly different than 1.00. Regression statistics ($r = 0.68$; $p = 5.2 \times 10^{-18}$) are also the same for all values of C_B. The only difference is reduction of the intercept A. In effect, decreasing values of C_B cause BCP_{Dil} estimates to converge on BCP_{Leu}. The whole regression moves vertically downward toward the 1 : 1 line in Fig. 1.

Table 1. Mean estimates for instantaneous rates of bacterial growth, grazing mortality and net growth and daily rates of BCP for experiments conducted at CCE stations with low, intermediate, and high near-surface values of PP.

Surface PP (mg C m^{-3} d^{-1})			
Variable	PP < 10	10 > PP > 100	PP > 100
Measurements (*n*)	44	34	47
Mean PP (mg C m^{-3} d^{-1})	3.3 ± 0.4	15.6 ± 3.3	133 ± 28
Growth rate, μ (d^{-1})	0.23 ± 0.02	0.42 ± 0.04	0.62 ± 0.05
Grazing mortality, m (d^{-1})	0.27 ± 0.04	0.38 ± 0.05	0.49 ± 0.05
Net growth, k (d^{-1})	−0.04 ± 0.02	0.04 ± 0.04	0.14 ± 0.03
BCP$_{Dil}$ (mg C m^{-3} d^{-1})	1.71 ± 0.20	5.82 ± 0.78	12.16 ± 1.34
BCP$_{Leu}$ (mg C m^{-3} d^{-1})	0.86 ± 0.07	2.36 ± 0.31	5.85 ± 0.81

Instantaneous rates and BCPDil are from dilution experiments. BCPLeu are from matched (day, depth) incubations for 3H-leucine uptake. Uncertainties are SEM values.

Lastly, we examined where values of BCP$_{Leu}$ reside with respect to BCP$_{Min}$ estimates derived simply from the positive net changes in bacterial cell abundance measured over 24-h incubations. As suggested by the low average net changes in experiments (*k* values in Table 1), the experiments divide fairly evenly between those with positive (*n* = 70) and negative (*n* = 55) net growth rates. Negative results are shown as 0.01 mg C m^{-3} d^{-1} in Fig. 4 and not further considered. Of

Fig. 4. Comparison of minimum estimates of BCP$_{Min}$ determined from net growth of bacteria cells in 24-h incubations to experimentally estimated production from ^{3}H-leucine assays (BCP$_{Leu}$). All dilution experiments with negative net growth rates of bacteria are plotted at BCP$_{Min}$ = 0.01 mg C m^{-3} d^{-1}.

the 70 positive results, 29 (41%) exceed their corresponding BCP$_{Leu}$ estimates, and a substantial number of other BCP$_{Min}$ values are close to the 1 : 1 line. In general, the higher BCP$_{Min}$ estimates conform to the 1 : 1 line with BCP$_{Leu}$ despite the fact that they do not include any consideration for bacterial production losses to grazing, viral lysis or other processes during the 24-h incubations.

Discussion

Given that the CCE spans a large productivity gradient from oligotrophic open ocean to coastal upwelling, the most important result of our method comparison is that BCP$_{Dil}$ follows the general trend in BCP$_{Leu}$ without any obvious systematic bias relating to system richness. There is, however, a factor-of-two difference in the raw BCP results. In the discussion below, we consider the various factors that contribute to this rate difference and try to resolve the offset. In addition, we highlight areas where combined results of dilution and ^{3}H-leucine techniques can be used to mutual advantage.

Methodological uncertainties

Dilution and ^{3}H-leucine methods arrive at BCP estimates by very different approaches that have no direct measurements in common. Dilution takes a population dynamic approach that involves the vital growth rate μ and three variables (cell abundance, P_0; cell carbon content, C_B; and net
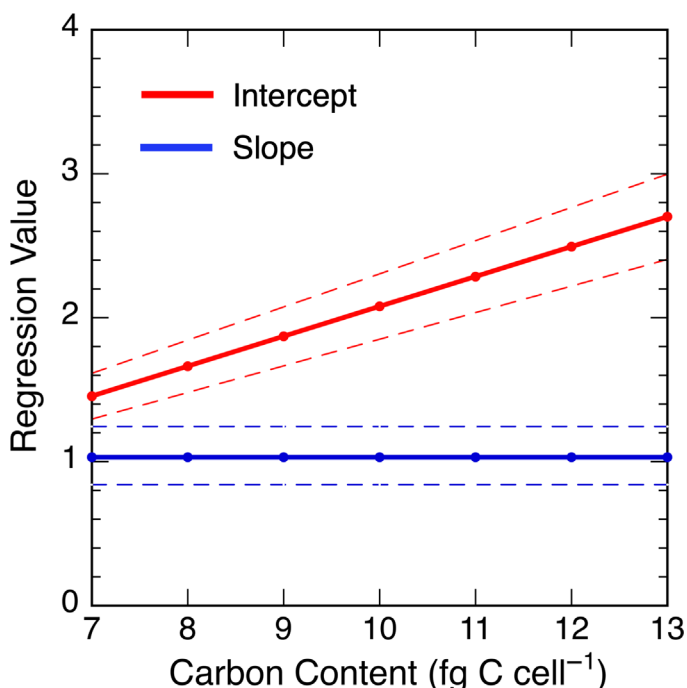

Fig. 3. Results of sensitivity analysis of regression variables (intercept, slope) for BCP$_{Dil}$ (Y) relative to BCP$_{Leu}$ (X) for different values of bacterial cell carbon applied to all dilution results. Dashed lines are upper and lower 95% confidence limits for Model II regressions.
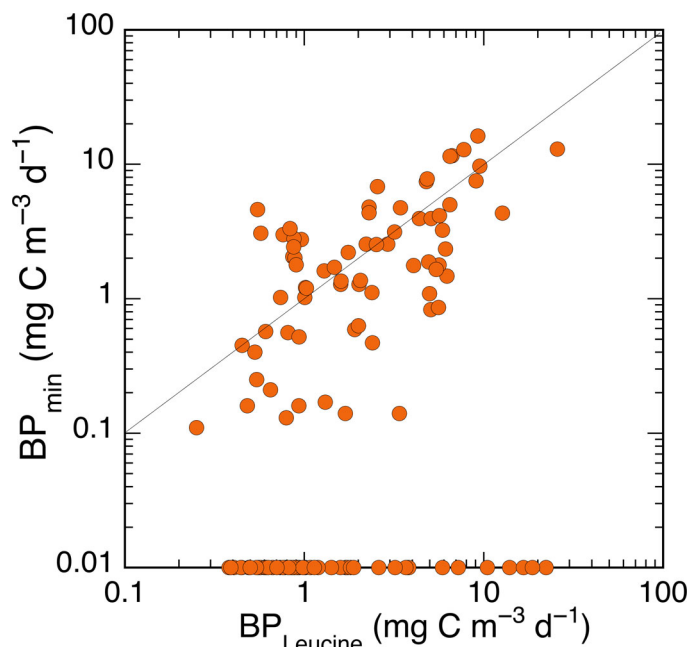
growth rate, k) that determine the mean population biomass to which μ applies. ^{3}H-leucine measures the uptake of the isotopically labeled substrate into protein, which is multiplied by a carbon conversion factor (CF_{Leu}) to compute BCP.

For BCP_{Dil}, k has a negligible systematic impact on CCE production calculations because the mean value is close to zero (Table 1). FCM provides high-precision bacterial counts for P_0 and the underlying the calculations of μ and is, therefore, also an unlikely source of substantial error. The efficacy of FCM counts is demonstrated by the close agreement between initial P_0 in dilution bottles and the relative volumes of filtered and natural seawater added (i.e., 0.1-μm filtration removes DNA-containing particles identified as bacteria with $\sim$ 99% efficiency). In contrast, C_B has substantial uncertainties, discussed separately below. That leaves μ as the only variable determined by the dilution manipulation per se (k comes from undiluted bottles) and therefore subject to the general methodological assumptions (e.g., exponential rates and linear response to dilution; Landry 1993). For phototrophs, results from two-bottle dilution experiments in the CCE and central Pacific have been found to be consistent with measured net changes of the ambient phytoplankton community (Landry et al. 2009, 2011), with contemporary measurements of PP by ^{14}C uptake (Landry et al. 2011) and cross-shelf variability of [234]thorium-based particle export (Stukel et al. 2011), and they provide the basis for inverse models that fit with many other independently measured variables (Landry et al. 2020). The main concern for application of the method to heterotrophic osmotrophs is the potential enrichment of dissolved organic substrates from the filtration process (Fuhrman and Bell 1985; Pree et al. 2016), which would alter the growth environment in the dilution treatment and overestimate μ. In other respects, the manipulation should be relatively neutral for bacteria because phytoplankton production of dissolved substrates, carbon demand of the bacterial community, and mortality losses to grazers are all reduced proportionately by dilution. Lacking clear evidence either for or against substrate enrichment of filtrate, it could well be an explanation for the BCP_{Dil} vs. BPC_{Leu} rate offset, though it would be surprising to be uniform across a broad trophic gradient and does not explain why BCP_{Min} exceeds BPC_{Leu} in a large proportion of experiments. As discussed below, the explanation is more likely the estimate of bacteria cell C.

For BCP_{Leu}, we used the theoretical maximum value for CF_{Leu}, which includes the factor of 2 for isotope dilution of the internal cell leucine pool (Simon and Azam 1989, Simon 1991). We believe this conversion factor is justified by the very short incubation duration (specific activity of internal pools cannot adjust instantaneously), but it is a maximum that cannot be adjusted higher to explain the BCP offset. Underestimates of BCP_{Leu} might however arise from unnatural incubation conditions or from inefficiencies in recovering ^{3}H-labeled protein through the decanting, centrifugation and rinsing steps. With regard to incubation conditions, Church

et al. (2004) observed that rates of ^{3}H-leucine uptake in the central Pacific were 48–92% higher in the light than in the dark, but they could not exclude photoheterotrophy by *Prochlorococcus* as a contributing factor to this difference. With regard to label recovery, Pace et al. (2004) documented that ^{3}H-leucine uptake results for different brands of microcentrifuge tubes varied by 30% in general and up to almost a factor 2 in the extreme. While we do not invoke such factors to reconcile differences between BCP_{Dil} and BPC_{Leu} rates in the present study, it is nonetheless important to recognize that factor-of-two uncertainties may apply to either method.

Carbon content of bacteria

Estimates of bacteria cell carbon in the ocean vary by more than an order of magnitude from $\sim$ 2 to 30 fg C cell^{-1} (Lee and Fuhrman 1987; Pomroy and Joint 1999; Gundersen et al. 2002; Rappé et al., 2002). The range of values that we used, 8–11 fg C cell^{-1}, were based on microscopical measurements and are representative of mid-range estimates that have been applied broadly (Fukuda et al. 1998; Ducklow 2000; Garrison et al. 2000). Here, however, we consider several ways in which the circumstances of those measurement may have overestimated cell C values by significant amounts.

The first issue is the choice of equation to convert cell BV to carbon, with the relationship $C_B = 120 \times BV^{0.72}$ of Norland (1993) being, in retrospect, perhaps a better alternative to the earlier equation of Simon and Azam (1989), which we used initially in this study. These relationships produce similar estimates of C_B for relatively large cells (0.7 μm) in the size range of *Prochlorococcus*, but diverge for smaller cells. For BV values that give 8–11 fg C cell^{-1} in the Simon and Azam (1989) equation, the C_B range would be 5.6–8.5 fg C cell^{-1} with the Norland (1993) relationship. Gundersen et al. (2002) determined an even lower BV to carbon relationship, $C_B = 108.8 \times BV^{0.898}$, for open-ocean subtropical waters based on single-cell measurements by X-ray microanalysis. For the 0.025–0.042 μm^3 size range that includes most bacteria of the Sargasso Sea, that relationship gives values of 4.0 to 6.3 fg C cell^{-1}.

The second issue in the present study is that cell abundance estimates from the samples used to estimate cell BV by microscopy accounted for only 60% on average of the bacterial abundances measured by FCM. If the missing counts are smaller cells, either dimly stained or passing through the 0.2-μm filter, a reasonable assumption might be that they were half the C content of those that were measured. To correct for undercounting of smaller cells, a factor of 0.8 (= (0.6 × 1.0) + (0.4 × 0.5)) would then need to be applied, bringing the C_B range to 4.5–6.8 fg C cell^{-1} based on the Norland (1993) equation.

The third issue is that measuring bacteria cell size at midday, during the peak hours of organic substrate availability, likely introduces time-of-day bias relative to mean cell size for our pre-dawn experiments. We quantified this difference by comparing the values of bead-normalized FALS, an index

of relative size for submicron particles, from FCM analyses of 02:00 and 11:00 hydrocasts for the two cruises (P1604, P1708) with microscopical size estimates. FALS results differ by a factor of 0.84 ($FALS_{0200} = 0.836 \pm 0.009$; $FALS_{1100} = 0.992 \pm 0.006$), which corresponds to a correction factor of 0.91 for cell C following the power 0.55 relationship of DuRand and Olson ([1996](#)). This reduces our operative cell size range to 4.1–6.2 fg C cell^{-1}. The analysis revealed no difference in mean bacteria FALS between initial and final samples from dilution incubations, consistent with balanced cell growth over 24 h. However, bead-normalized Side Scatter (SS), an index of cell granularity, showed much larger time-of-day differences than FALS ($SS_{0200} = 0.140 \pm 0.007$; $SS_{1100} = 0.321 \pm 0.017$), suggesting that cells at midday were in a different division state or possibly showing signs of viral infection. Using the same bead-normalized FALS comparisons, we found little indication of cell size difference for samples collected at 02:00 at low and high productivity stations (0.82 ± 0.02 vs. 0.81 ± 0.01, respectively), which were more similar to one another than to samples collected 9 h later (midday) in the same water masses following the drogued drifter.

The above results suggest that an intermediate value of ~5 fg C cell^{-1} might apply equally well as an average early morning minimum estimate of bacteria cell size irrespective of differences in station productivity. This FCM-informed value is within the size range previously suggested for bacteria in the oligotrophic open ocean (Christian and Karl [1994](#); Gundersen et al. [2002](#)) and measured for SAR11 cultures (White et al. [2019](#)). We reanalyzed BCP_{Dil} based on constant 5 fg C cell^{-1} and plot them relative to BCP_{Leu} in Fig. [5](#). It follows from the sensitivity analysis in Fig. [3](#) that reducing C_B by about a factor of 2 on average aligns BCP_{Dil} rates to where they fit closely to the 1 : 1 line with BCP_{Leu} (Fig. [5a](#)). Reduced

bacteria cell C also moves most of the BCP_{Min} estimates below values that exceed BCP_{Leu} (Fig. [5b](#)).

Contemporary issues for BCP measurements

We consider here the relevance of our method comparison results relative to recent suggestions that the bacterial cell division rates may be grossly underestimated in the open ocean (Popendorf et al. [2020](#)), that BCP_{Leu} rates may be grossly overestimated in the open ocean (Giering and Evans [2022](#)), and the more general problem of assessing bacterial losses to viral lysis. Popendorf et al. ([2020](#)) measured turnover estimates of bacterial phospholipids suggesting cell growth rates of ~0.80 d^{-1} in oligotrophic subtropical waters of the Atlantic and Pacific Ocean, which were seven-fold higher than growth rates determined by ^{3}H-leucine. They partially explained the discrepancy by invoking a smaller value of C_B, arriving at the same 5 fg C cell^{-1} estimate that we did, although there would still be a substantial impact on current understanding of bacterial growth efficiency (BGE) and carbon demand to meet the remaining growth rate difference. Here, we note that the principal measurement to determine BCP_{Dil} is the growth rate μ of bacterial cells, which is independent of the cell biomass applied or the vagaries of BGE or carbon demand. Our estimates of μ for bacterial cells are >three-fold lower than the phospholipid estimates for open ocean waters (0.23 ± 0.02 d^{-1}; Table [1](#)), and even lower than open-ocean phospholipid rates on average in high productivity coastal waters (0.62 ± 0.05 d^{-1}). Ecologically, it seems highly unlikely that small bacteria would be growing faster on average than substantially larger phototrophic bacteria like *Prochlorococcus*, if the main loss term is direct interception grazing by shared size-selective flagellates, for which mortality scales to cell radius (Monger and Landry [1991](#), [1992](#)). For an assumed C_B value of 5 fg C cell^{-1}, our dilution results directly support estimates of bacterial μ derived from ^{3}H-
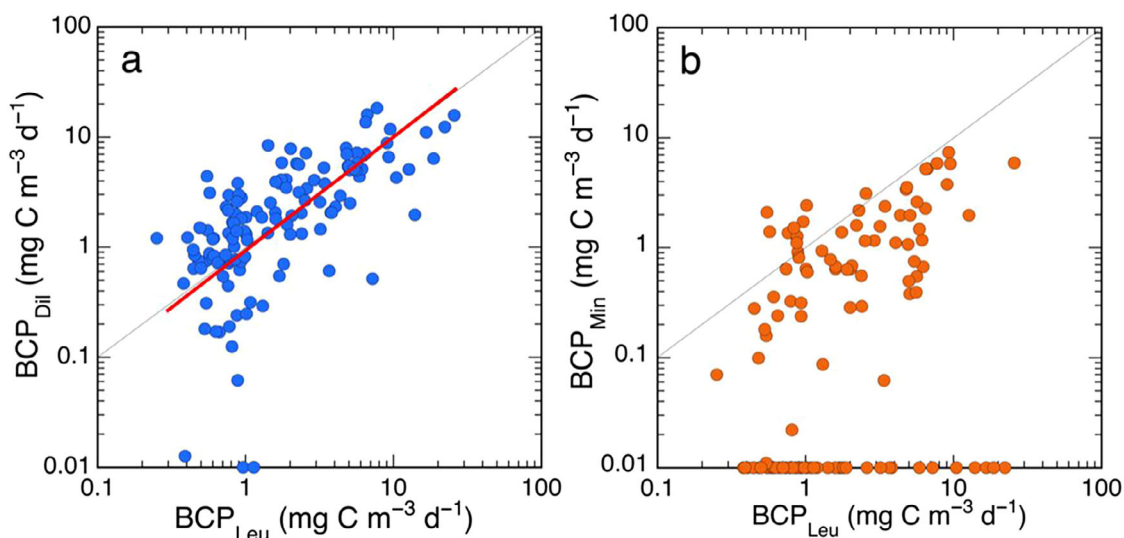

Fig. 5. Reanalysis of BCP rate comparisons for constant bacteria cell carbon content of 5 fg C. All other factors as in Figs. [1](#) and [4](#).

leucine $(0.21 \pm 0.01 \, \mathrm{d}^{-1})$ for low productivity CCE waters. An important caveat to our dilution-based estimates, however, is that they do not account for the component of bacterial growth that is lost to viral lysis. This is because the standard 0.1- or 0.2-μm filters used to make filtered water for the dilution treatments are too coarse to dilute viruses as a mortality agent. As shown by Baudoux et al. (2008) and Pasulka et al. (2015) and others, viral impacts can be measured and compared to standard dilution growth-grazing results by a modified approach that uses 30-kDa filtered water.

Giering and Evans (2022) have argued that the commonly used theoretical value of CF_{Leu}, 3.1 kg C (mol Leu)$^{-1}$, is more than a factor of 6 too high for the open ocean. To put that argument in a growth rate context, our BCP_{Leu} results for low production waters using high CF_{Leu} and initial 8 fg C cell^{-1} estimates give growth rates of $\sim 0.1 \, \mathrm{d}^{-1}$, or about one cell division per week. A > six-fold reduction of such rates would therefore mean one bacterial cell division every 1.5 months in waters where cooccurring phototrophic bacteria grazed by a shared assemblage of small flagellate predators (Kuipers and Witte 2000; Taylor and Landry 2018; Follet et al. 2022) are dividing at rates closer to once per day. This ecologically unrealistic result would clearly also not fit the inferences of high bacterial turnover rates from phospholipid analyses (Popendorf et al. 2020). As noted above, the parsimonious fit of independently measured BCP_{Dil} and BCP_{Leu} for $C_B = 5$ fg C cell^{-1} provides some support for the high theoretical estimate of CF_{Leu} that we used in this study, which appears to apply equally well across the broad trophic gradient of the CCE.

Lastly, in conducting our method intercomparison, we expected that BCP_{Leu} would need to exceed BCP_{Dil} because the latter does not account for losses to viruses, which are believed to be about equally important to grazing as a bacterial mortality factor (Proctor and Fuhrman 1990; Fuhrman 1999). If BCP_{Leu} and BCP_{Dil} rates are indeed similar, however, BCP_{Leu} measurements must also miss all or most of the portion of production shunted to the dissolved pool by viral mortality (Fuhrman 1999; Suttle 2007). Given that protein comprises a large portion of viral mass, this would imply that leucine uptake into viral infected cells would have to be diminished during uptake incubations or any products of viral lysis inefficiently recovered by centrifugation or its 0.2-μm filtration alternative. Such a blanket loss of viral signal may seem farfetched. Nonetheless, viral lytic cycles are observed to occur in the oceans on diel cycles around the onset of darkness (Aylward et al. 2017; Ho et al. 2021) and could be triggered by dark incubation conditions of ^{3}H-leucine assays. Alternatively, calibration grow-out dilution cultures may discount viral losses (similar to standard growth-grazing dilution experiments), or TCA addition to stop the experiments might not prevent membrane lysis of infected cells. We mention these possibilities to highlight one scenario in which dilution, ^{3}H-leucine and phospholipid turnover inferences might provide

mutually compatible information about bacterial production rates—if phospholipid turnover accounted for additional losses to viruses, while the other two methods did not.

Comments and recommendations

The present method comparison was not undertaken to advance the dilution technique as a generally equivalent approach to ^{3}H-leucine for assessing bacterial production in marine ecosystems. While ^{3}H-leucine is not without its issues, it is a more direct method for that measurement, and its long-term usage as the methodological standard allows clearer intercomparisons of ecosystem influences of BCP rates in current, future and historical studies. The dilution technique does, however, offer a distinct advantage for integrating bacteria into a broader food web context by providing estimates of their growth and grazing mortality rates in the same incubations that measure the growth and grazing of phototrophic microbes (*Prochlorococcus*, *Synechococcus*, picoeukaryotes) as well as other phytoplankton (e.g., Landry et al. 2022a). The expanding usage of sequence analyses with dilution experiments to resolve species- and clade-specific differences in growth and grazing dynamics (Yokokawa and Hagata 2005; Cheung et al. 2022) can also be expected to amplify this advantage in the future. It is therefore useful to know that BCP_{Dil} results can be compatible with BCP_{Leu}, given appropriate attention to bacteria cell carbon content. Our results demonstrate that a mean C_B of 5 fg C cell^{-1} brings BCP_{Dil} and BCP_{Leu} in line with one another over the broad range of CCE productivity conditions. This knowledge informs future CCE studies and may be applicable to other systems as well.

While it may be obvious from the equation for BCP_{Dil} calculation (Eq. 4) that bacteria cell C content has a direct multiplicative impact on the rate results, the large uncertainties around C_B did not quite hit home until the present analysis. Thus, regardless of how carefully dilution experiments are prepared, how closely they adhere to the assumptions of the method or how scrupulously they are incubated under natural in situ conditions, their BCP_{Dil} results can be no better than the estimates of C_B, for which literature assumptions and calculations differ greatly. This issue applies equally to any use of C_B to derive an estimates of bacterial growth rate μ from BCP_{Leu}. Additionally, diel variability of bacteria cell size has now been shown to influence the intercomparison of results for processes measured on cruises at different times of day. FCM provides a rapid and efficient method for measuring bacterial abundances and indices of cell size. What the field needs is a standardized calibrated FCM approach (e.g., specific-bead standards and protocols) that can be used with different instruments to assess mean cell sizes and carbon contents in natural samples.

Lastly, with regard to specific methodological recommendations, it is sobering that current literature, four decades after Azam et al. (1983), suggests a > 40-fold range of uncertainty

for bacterial growth rates in the open ocean (Popendorf et al. 2020; Giering and Evans 2022). By comparison, our efforts to resolve a two-fold difference in BCP rates seem trivial. A previous study (Pree et al. 2016) recommended that ^{3}H-leucine incubations be done in conjunction with dilution incubations as a form of control to assess whether μ estimates are influenced by added organics in filtrated water. Having done that exercise after a fashion here, we now recommend exactly the opposite—that dilution experiments be done to support BCP_{Leu}. This recommendation follows from the fact that μ is not directly measured by BCP_{Leu} but must be derived using a poorly known C_B that can be varied within a broad range by assumption or choice of BV relationship. Standard BCP_{Leu} calibration cultures also involve unnatural separation of bacteria from ambient concentrations of primary producers, size-selective grazers and delivery rates of labile organics, which add to other uncertainties in internal pool dilution factors and leucine diversion to other metabolic uses (Giering and Evans 2022). In contrast, since μ is a primary product of the dilution manipulation computed directly from measured changes in bacteria cell abundances, it provides an independent measurement constraint on BCP_{Leu} results. Dilution and ^{3}H-leucine experiments seem compatible in this regard, with each providing a critical piece (μ vs. BCP) more directly than the other, which together can constrain estimates of bacterial biomass and C_B. Even where they disagree, jointly run dilution and ^{3}H-leucine assays will help to narrow the range of actual uncertainties in bacterial stocks and rates.

Data availability statement

Data for BCP comparison regression relationships are provided in Table S1. Relevant environmental data are available by cruise, CTD number, and sampling depth at CCE data website *https://oceaninformatics.ucsd.edu/datazoo/catalogs/ccelter/datasets*.

References

Aylward, F. O., and others. 2017. Diel cycling and long-term persistence of viruses in the ocean's euphotic zone. Proceedings of the National Academy of Sciences of the United States of America **114**: 11446–11451. 10.1073/pnas.1714821114

Azam, F., T. Fenchel, G. J. Field, J. S. Gray, L. A. Meyer-Reil, and F. Thingstad. 1983. The ecological role of water-column microbes in the sea. Marine Ecology Progress Series **10**: 257–263. 10.3354/meps010257

Baudoux, A. C., M. J. W. Veldhuis, A. A. M. Noordeloos, G. van Noort, and C. P. D. Brussaard. 2008. Estimates of virus vs. grazing induced mortality of picophytoplankton in the North Sea during summer. Aquatic Microbial Ecology **52**: 69–82. 10.3354/ame01207

Bratbak, G. 1985. Bacterial biovolume and biomass estimations. Applied and Environmental Microbiology **49**: 1488–1493. doi:10.1128/aem.49.6

Calbet, A., and M. R. Landry. 2004. Phytoplankton growth, microzooplankton grazing and carbon cycling in marine systems. Limnology and Oceanography **49**: 51–57. doi:10.4319/lo.2004.49.1.0051

Cheung, S., and others. 2022. High biomass turnover rates of endosymbiotic nitrogen-fixing cyanobacteria in the western Bering Sea. Limnology and Oceanography Letter **7**: 501–509. doi:10.1002/lol2.10267

Christian, J. R., and D. M. Karl. 1994. Microbial community structure at the U.S.-Joint Global Ocean flux Study Station ALOHA: Inverse methods for estimating biochemical indicator ratios. Journal of Geophysical Research: Oceans **99**: 14269–14276. doi:10.1029/94JC00681

Church, M. J., H. W. Ducklow, and D. M. Karl. 2004. Dependence of ^{3}H-leucine Incorporation in the oligotrophic North Pacific Ocean. *Applied and Environmental Microbiology* **70**: 4079–4087. doi:10.1128/AEM.70.7.4079–4087.2004.

Ducklow, H. W. 2000. Bacterial production and biomass in the oceans, p. 85–120. *In* D. L. Kirchman [ed.], Microbial ecology of the oceans. Wiley-Liss.

DuRand, M. D., and R. J. Olson. 1996. Contributions of phytoplankton light scattering and cell concentration changes to diel variations in beam attenuation in the equatorial Pacific from flow cytometric measurements of pico-, ultra- and nanoplankton. Deep-Sea Research Part II: Topical Studies in Oceanography **43**: 891–906. doi:10.1016/0967-0645(96)00020-3

Follet, C. L., and others. 2022. Trophic interactions with heterotrophic bacteria limit the range of *Prochlorococcus*. Proceedings of the National Academy of Sciences of the United States of America **119**: e2110993118. doi:10.1073/pnas.2110993118

Fuhrman, J. A. 1999. Marine viruses and their biogeochemical and ecological effects. Nature **399**: 541–548. doi:10.1038/21119

Fuhrman, J. A., and T. M. Bell. 1985. Biological considerations in the measurement of dissolved free amino acids in seawater and implications for chemical and microbiological studies. Marine Ecology Progress Series **25**: 13–21. doi:10.3354/MEPS025013

Fukuda, R., H. Ogawa, T. Nagata, and I. Koike. 1998. Direct determination of carbon and nitrogen contents of natural bacterial assemblages in marine environments. Applied and Environmental Microbiology **64**: 3352–3358. doi:10.1128/aem.64.9.3352-3358.1998

Garrison, D. L., and others. 2000. Microbial food web structure in the Arabian Sea: A US JGOFS study. Deep-Sea Research Part II: Topical Studies in Oceanography **47**: 1387–1422. doi:10.1016/S0967-0645(99)00148-4

Giering, S. L. C., and C. Evans. 2022. Overestimation of prokaryotic production by leucine incorporation — And how to avoid it. Limnology and Oceanography **67**: 726–738. doi:10.1002/lno.12032

Gundersen, K., M. Heldal, S. Norland, D. A. Purdie, and A. H. Knap. 2002. Elemental C, N, and P cell content of individual bacteria collected at the Bermuda Atlantic time-series study (BATS) site. Limnology and Oceanography **47**: 1525–1530. doi:10.4319/lo.2002.47.5.1525

Ho, P.-C., G.-C. Gong, C.-H. Hsieh, P. W.-Y. Chen, and A.-Y. Tsai. 2021. Diel variation of viral production in a coastal subtropical marine system. Diversity **13**: 426. doi:10.3390/d13090426

Kirchman, D. 2001. Measuring bacterial biomass production and growth rates from leucine sincorporation in natural aquatic environments. Methods in Microbiology **30**: 227–237. doi:10.1016/S0580-9517(01)30047-8

Kirchman, D., E. K'nees, and R. Hodson. 1985. Leucine incorporation and its potential as a measure of protein synthesis by bacteria in natural aquatic systems. Applied and Environmental Microbiology **49**: 599–607. doi:10.1128/aem.49.3.599-607.1985

Kuipers, B. R., and H. J. Witte. 2000. Prochlorophytes as secondary prey for heterotrophic nanoflagellates in the deep chlorophyll maximum layer of the (sub)tropical North Atlantic. Marine Ecology Progress Series **204**: 53–63. doi:10.3354/meps204053

Kranz, S. A., and others. 2020. Lagrangian studies of marine production: A multimethod assessment of productivity relationships in the California current ecosystem upwelling region. Journal of Geophysical Research: Oceans **125**: e2019JC015984. doi:10.1029/2019jc015984

Landry, M. R. 1993. Estimating rates of growth and grazing mortality of photoautotrophic plankton by dilution, p. 715–722. *In* P. F. Kemp, B. F. Sherr, E. B. Sherr, and J. J. Cole [eds.], Handbook of methods in aquatic microbial ecology. Lewis Publishers. doi:10.1201/9780203752746-83

Landry, M. R., and R. P. Hassett. 1982. Estimating the grazing impact of marine micro-zooplankton. Marine Biology **67**: 283–288. doi:10.1007/BF00397668

Landry, M. R., L. W. Haas, and V. L. Fagerness. 1984. Dynamics of microbial plankton communities: Experiments in Kaneohe Bay, Hawaii. Marine Ecology Progress Series **16**: 127–133. doi:10.3354/meps016127

Landry, M. R., J. Kirshtein, and J. Constantinou. 1995. A refined FLB-dilution approach for measuring the community grazing impact of microzooplankton, with experimental tests in the equatorial Pacific. Marine Ecology Progress Series **120**: 53–63. doi:10.3354/meps120053

Landry, M. R., and others. 2003. Phytoplankton growth and microzooplankton grazing in high-nutrient, low-chlorophyll waters of the equatorial Pacific: Community and taxon-specific rate assessments from pigment and flow cytometric analyses. Journal of Geophysical Research **108**: 8142. doi:10.1029/2000JC000744

Landry, M. R., and others. 2008. Depth-stratified phytoplankton dynamics in cyclone opal, a subtropical mesoscale eddy. Deep-Sea Research Part II: Topical Studies in Oceanography **55**: 1348–1359. doi:10.1016/j.dsr2.2008.02.001

Landry, M. R., M. D. Ohman, R. Goericke, M. R. Stukel, and K. Tsyrklevich. 2009. Lagrangian studies of phytoplankton growth and grazing relationships in a coastal upwelling ecosystem off Southern California. Progress in Oceanography **83**: 208–216. doi:10.1016/j.pocean.2009.07.026

Landry, M. R., K. E. Selph, A. G. Taylor, M. Décima, W. M. Balch, and R. R. Bidigare. 2011. Phytoplankton growth, grazing and production balances in the HNLC equatorial Pacific. Deep-Sea Research Part II: Topical Studies in Oceanography **58**: 524–535. doi:10.1016/j.dsr2.2010.08.011

Landry, M. R., M. R. Stukel, and M. R. Décima. 2020. Food-web fluxes support high rates of mesozooplankton respiration and production in the equatorial Pacific. Marine Ecology Progress Series **652**: 15–32. doi:10.3354/meps13479

Landry, M. R., K. E. Selph, R. R. Hood, C. H. Davies, and L. E. Beckley. 2022a. Low temperature sensitivity of picophytoplankton P:B ratios and growth rates across a natural 10°C temperature gradient in the oligotrophic Indian Ocean. Limnology and Oceanography Letter **7**: 112–121. doi:10.1002/lol2.10224

Landry, M. R., and others. 2022b. Microbial community biomass, production and grazing along 110° E in the eastern Indian Ocean. Deep-Sea Research Part II: Topical Studies in Oceanography **202**: 105134. doi:10.1016/j.dsr2.2022.105134

Lee, S., and J. Fuhrman. 1987. Relationships between biovolume and biomass of naturally derived marine bacterioplankton. Applied and Environmental Microbiology **53**: 1298–1303. doi:10.1128/aem.53.6.1298-1303.1987

Legendre, P. 2022. Model II regression user's guide, R edition. https://cran.r-project.org/web/packages/lmodel2/vignettes/mod2user.pdf.

Lessard, E. J., and M. C. Murrell. 1998. Microzooplankton herbivory and phytoplankton growth in the northwestern Sargasso Sea. Aquatic Microbial Ecology **16**: 173–188. doi:10.3354/ame016173

Monger, B. C., and M. R. Landry. 1991. Prey-size dependency of grazing by free-living marine flagellates. Marine Ecology Progress Series **74**: 239–248. doi:10.3354/meps074239

Monger, B. C., and M. R. Landry. 1992. Size-selective grazing by heterotrophic nanoflagellates: An analysis using live-stained bacteria and dual-beam flow cytometry. Archiv für Hydrobiologie Beihefte Ergebnisse der Limnologie **37**: 173–185.

Monger, B. C., and M. R. Landry. 1993. Flow cytometric analysis of marine bacteria with Hoechst 33342. Applied and Environmental Microbiology **59**: 905–911. doi:10.1128/aem.59.3.905-911.1993

Morrow, R., M. D. Ohman, R. Goericke, T. B. Kelly, B. M. Stephens, and M. R. Stukel. 2018. CCE V: Primary production, mesozooplankton grazing, and the biological pump in the California current ecosystem: Variability and response to El Niño. Deep-Sea Research Part I: Oceanographic Research **140**: 52–62. doi:10.1016/j.dsr.2018.07.012

Norland, S. 1993. The relation between biomass and volume of bacteria, p. 303–308. *In* P. Kemp, B. F. Sherr, E. B. Sherr, and J. J. Cole [eds.], Handbook of methods in aquatic microbiology. Lewis Publishers. doi:10.1201/9780203752746-36

Pace, M. L., P. del Giorgio, D. Fischer, R. Condon, and H. Malcom. 2004. Estimates of bacterial production using the leucine incorporation method are influenced by differences in protein retention of microcentrifuge tubes. Limnology and Oceanography Methods **2**: 55–61. doi:10.4319/lom.2004.2.55

Pasulka, A. L., T. J. Samo, and M. R. Lamdry. 2015. Grazer and viral impacts on microbial growth and mortality in the southern California current ecosystem. Journal of Plankton Research **37**: 1–17. doi:10.1093/plankt/fbv011

Pomroy, A., and I. Joint. 1999. Bacterioplankton activity in the surface waters of the Arabian Sea during and after the 1994 SW monsoon. Deep-Sea Research Part II: Topical Studies in Oceanography **46**: 767–794. doi:10.1016/S0967-0645(98)00127-1

Popendorf, K. J., M. Koblížek, and B. A. S. Van Mooy. 2020. Phospholipid turnover rates suggest that bacterial community growth rates in the open ocean are systematically underestimated. Limnology and Oceanography **65**: 1876–1890. doi:10.1002/lno.11424

Pree, B. C., and others. 2016. A simple adjustment to test reliability of bacterivory rates derived from the dilution method. Limnology and Oceanography Methods **14**: 114–123. doi:10.1002/lom3.10076

Proctor, L. M., and J. A. Fuhrman. 1990. Viral mortality of marine bacteria and cyanobacteria. Nature **343**: 60–62. doi:10.1038/343060a0

Rappé, M. S., S. A. Connon, K. L. Vergin, and S. J. Giovannoni. 2002. Cultivation of the ubiquitous SAR11 marine bacterioplankton clade. Nature **418**: 630–633. doi:10.1038/nature00917

Schmoker, C., S. Hernández-León, and A. Calbet. 2013. Microzooplankton grazing in the oceans: Impacts, data variability, knowledge gaps and future directions. Journal of Plankton Research **35**: 691–707. doi:10.1093/plankt/fbt023

Selph, K. E., and others. 2011. Spatially-resolved taxon-specific phytoplankton production and grazing dynamics in relation to iron distributions in the equatorial Pacific between 110 and 140° W. Deep-Sea Research Part II: Topical Studies in Oceanography **58**: 358–377. doi:10.1016/j.dsr2.2010.08.014

Simon, M. 1991. Isotope dilution of intracellular amino acids as a tracer of carbon and nitrogen sources of marine planktonic bacteria. Marine Ecology Progress Series **74**: 295–301. doi:10.3354/meps074295

Simon, M., and F. Azam. 1989. Protein-content and protein-synthesis rates of planktonic marine-bacteria. Marine Ecology Progress Series **51**: 201–213. doi:10.3354/meps051201

Smith, D. C., and F. Azam. 1992. A simple, economical method for measuring bacterial protein synthesis in seawater using ³H-leucine. Marine Microbial Food Webs **6**: 107–114.

Stukel, M. R., M. R. Landry, C. R. Benitez-Nelson, and R. Goericke. 2011. Trophic cycling and carbon export relationships in the California current ecosystem. Limnology and Oceanography **56**: 1866–1878. doi:10.4319/lo.2011.56.5.1866

Suttle, C. A. 2007. Marine viruses—Major players in the global ecosystem. Nature Reviews Microbiology **5**: 801–812. doi:10.1038/nrmicro1750

Taylor, A. G., and M. R. Landry. 2018. Phytoplankton biomass and size structure across trophic gradients in the southern California current and adjacent ocean ecosystems. Marine Ecology Progress Series **592**: 1–17. doi:10.3354/meps12526

Valencia, B., M. R. Stukel, A. E. Allen, J. P. McCrow, A. Rabines, and M. R. Landry. 2022. Microbial communities associated with sinking particles across an environmental gradient from coastal upwelling to the oligotrophic ocean. Deep-Sea Research Part I: Oceanographic Research **179**: 103668. doi:10.1093/plankt/fbab020

White, A. E., S. J. Giovannoni, Y. Zhao, K. Vergin, and C. A. Carlson. 2019. Elemental content and stoichiometry of SAR11 chemoheterotrophic marine bacteria. Limnology and Oceanography Letter **4**: 44–51. doi:10.1002/lol2.10103

Yokokawa, T., and T. Nagata. 2005. Growth and grazing mortality rates of phylogenetic groups of bacterioplankton in coastal marine environments. Applied and Environmental Microbiology **71**: 6799–6807. doi:10.1128/AEM.71.11.6799–6807.2005

Conflict of Interest

None declared